

Lawrence Berkeley National Laboratory

Recent Work

Title

PHOTOEFFECTS IN Fe₂O₃ SINTERED SEMICONDUCTORS

Permalink

<https://escholarship.org/uc/item/4sh3x7m2>

Author

Mcgregor, K.G.

Publication Date

1978-02-01

PHOTOEFFECTS IN Fe_2O_3 SINTERED SEMICONDUCTORS

K. G. McGregor, M. Calvin and J. Otvos

RECEIVED
LAWRENCE
BERKELEY LABORATORY

February 1978

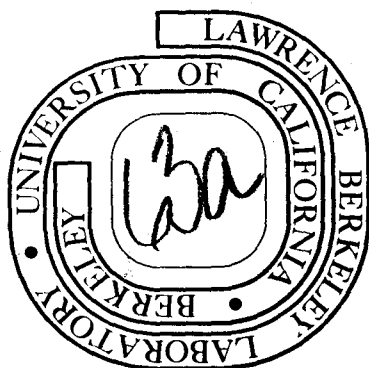
MAR 14 1978

LIBRARY AND
DOCUMENTS SECTION

Prepared for the U. S. Department of Energy
under Contract W-7405-ENG-48

TWO-WEEK LOAN COPY

*This is a Library Circulating Copy
which may be borrowed for two weeks.
For a personal retention copy, call
Tech. Info. Division, Ext. 5716*



DISCLAIMER

This document was prepared as an account of work sponsored by the United States Government. While this document is believed to contain correct information, neither the United States Government nor any agency thereof, nor the Regents of the University of California, nor any of their employees, makes any warranty, express or implied, or assumes any legal responsibility for the accuracy, completeness, or usefulness of any information, apparatus, product, or process disclosed, or represents that its use would not infringe privately owned rights. Reference herein to any specific commercial product, process, or service by its trade name, trademark, manufacturer, or otherwise, does not necessarily constitute or imply its endorsement, recommendation, or favoring by the United States Government or any agency thereof, or the Regents of the University of California. The views and opinions of authors expressed herein do not necessarily state or reflect those of the United States Government or any agency thereof or the Regents of the University of California.

PHOTOEFFECTS IN Fe_2O_3 SINTERED SEMICONDUCTORS

K. G. McGregor, M. Calvin, and J. Otvos

Laboratory of Chemical Biodynamics

Lawrence Berkeley Laboratory

University of California

Berkeley, California 94720

ABSTRACT

Polycrystalline sintered pellets of $\alpha\text{-Fe}_2\text{O}_3$ have been studied by capacitance and photoelectrochemical techniques. The pellets exhibit (i), photocurrent saturation at a given wavelength with increasing applied voltage, (ii), large dark currents at low applied voltage ($0.76 \mu\text{A cm}^{-2}$ at $+0.2 \text{ v.SCE}$), (iii), cathodic and anodic photocurrent transients at low levels of monochromatic irradiation, (iv), photocurrent onset at photon energies greater than 2.1 eV and (v), flat band potentials of -0.67 v. SCE at $\text{pH} = 14$. Capacitance measurements followed a Mott-Schottky relationship indicating a predominance of the semiconductor space charge layer over surface states and electrolyte effects. No degradation of the semiconductor properties could be observed at $\text{pH} = 4$.

INTRODUCTION

Interest in the production of hydrogen and oxygen utilizing the solar spectrum and semiconductor electrodes has led to a search for anodically stable semiconductor electrodes with a low band gap (2.0 eV)¹⁻¹¹. The generation of the electron-hole pair in n-type semiconductor surfaces by visible radiation results, under anodic polarization, in a movement of the electron into the bulk of the semiconductor leaving the hole at the semiconductor surface. The hole can either react with a species in the electrolyte e.g. H₂O and produce oxygen or it can react with a component of the semiconductor e.g. X⁻ and produce X with a degradation of the semiconductor surface layer. The latter process is by no means satisfactory, the degradation of the surface layer of the semiconductor resulting in poorer optical response due the accumulation of an optically dense material (S in CdS) or material loss from the semiconductor (Si). The hole left in the semiconductor surface must react with a species in the electrolyte and this species should, under ideal conditions, be water itself.

Semiconductor electrodes e.g. TiO₂^{12,13}, SrTiO₃¹⁴ have been shown to be able to produce oxygen upon illumination under anodic polarization. However, all such semiconductors have band gaps of 3.0 eV or greater and so require UV radiation to produce the electron-hole pair. When attempting to use the solar spectrum, this wavelength response is far from satisfactory and so attempts to find an anodically stable small band gap semiconductor have been initiated.

One such material which has shown promise is Fe₂O₃ with a band gap of 2.2 eV. It has been shown to be anodically stable^{5,6,9,15}. Studies of both single crystals⁵ and thin films^{6,9,15} of Fe₂O₃ have shown that the onset of the photocurrent does occur at approximately 2.0 eV and that for pH greater than 4, the photocurrent shows no deterioration under anodic

polarization even after several hours continuous operation and many experiments over several weeks. We report here the investigations carried out on polycrystalline Fe_2O_3 sintered semiconductors.

When a semiconductor electrode is contacted by an electrolyte¹⁶, an equilibrium is established in the system which is determined by the electron affinity of the semiconductor and the reduction potential of the reacting species in the solution. Surface states on the semiconductor may affect the equilibrium. The electron affinity and the reduction potential of the electrolyte thus determines the amount of band bending between the bulk of the semiconductor and the semiconductor surface at equilibrium. For highly doped semiconductors the Fermi level of the semiconductor and the conduction band level are considered to be isoenergetic so that the amount of band bending near the semiconductor surface is the difference between the conduction band before the establishment of the equilibrium and the flat band potential E_{FB} ; a measure of the conduction band of the semiconductor surface after equilibrium is established.

The capability of a given semiconductor electrode to drive a given reduction reaction is determined by the amount of band bending. If the band bending is too small, additional external biasing of the electrode will be needed to enable the chemical reaction to proceed. From capacitance measurements, values of the flat band potential can be obtained and hence decisions as to whether or not a chemical reaction will proceed at the electrode can be made. We measure the flat band potential for polycrystalline Fe_2O_3 sintered semiconductors and comment on the feasibility of hydrogen and oxygen production at this single electrode. It has been shown^{2,3} that, for the photoelectrolysis of water, a suitable photoanode should have a flat band potential at least as negative as that for SrTiO_3 i.e. $-1.2 \text{ v} \cdot \text{SCE}$ at $\text{pH} = 13.6$.

EXPERIMENTAL

Sintered pellets of Fe_2O_3 were prepared by the standard ceramic technique and was similar to the procedure used by Morin¹⁷. The Fe_2O_3 (Allied Chemical Reagent Grade) powder was mixed with TiO_2 powder (Allied Chemical Reagent Grade) in known Ti/Fe atomic ratios by wetting both powders with doubly distilled water and agitating the resulting slurry vigorously for 30 minutes. The slurry was then dried at 60-70°C at 500 torr and the resulting dry powder was crushed. The mixed powder was pelleted at 1500 kg cm^{-2} into pellets of typical dimensions 1.3 cm (diameter) x 0.1 cm (thick). The pressed pellet was fired at 1100°C for 16 hrs. in air. The resulting Fe_2O_3 polycrystalline pellet was black with resistivities varying from $1000 \Omega\text{-cm}$ to $10^{10} \Omega\text{-cm}$ depending on the Ti content of the original powder. The higher the atomic % Ti, the lower the resistivity. The samples were n-type as determined by both photoelectrochemical and capacitance measurements.

Electrical contacts to the Fe_2O_3 pellets was made with Ag epoxy on one side as an ohmic contact and the electrolyte on the other. The photoelectrochemical cell (PEC) and accompanying equipment used in this work is shown in Fig. 1. The reference electrode was a saturated calomel electrode and the counter electrode was a carbon rod. The exposed semiconductor surface area in all experiments was 0.071 cm^2 . The Fe_2O_3 was sealed to a black plexiglass support by gray Silicone Adhesive (RTV 3145 Dow Corning) and the support mounted in the pyrex PEC cell. The window of the cell was quartz glass.

Current-voltage measurements were recorded with a PAR 173 Potentiostat and a PAR 179 Digital Coulometer. The light was a 450 Watt Xenon arc which was monochromatized with a Bausch and Lomb 33-86-02 Visible Monochromator. For wavelength greater than 500 nm, a Corning CS3-73 colored glass filter

was used to remove light of the second order. The entrance to exit slit ratio was set at 1.8 with an exit slit of 2 mm and a resulting bandwidth of 12.8 nm. Photocurrents were recorded every 20 nm from the onset of the photocurrent at 600 nm to 360 nm.

As shown in Fig. 1, the light path was split and a sample beam passed to a photomultiplier tube (PMT) with a 200-600 nm spectral response (RCA 6903) which together with suitable filters allowed a monitoring of the irradiance on the semiconductor when mounted in the PEC cell at any time during the experiment. Fluctuations of the source irradiance could then be corrected for in all photocurrent measurements. Typical irradiances were 1.06 mW cm^{-2} at 520 nm corresponding to $2.8 \times 10^{15} \text{ photons s}^{-1} \text{ cm}^{-2}$. To further improve the stability of the calibration data, the reference light beam was modulated at a fixed frequency and the signal detected with a PAR 120 lock-in amplifier. This ensured that dark drifts in the PMT would not shift the values of the irradiance. The initial calibration of the PMT was carried out using a Hewlett-Packard Radiant Flux Meter (8330A) and Detector (8334A) with the detector mounted in the position of the PEC cell.

Capacitance measurements were carried out using an external bias (Heath Reference Voltage Source), a 1650A General Radio Company Universal bridge with an internal 1 kHz oscillator and a Keithley 151 Microvoltmeter. The voltage source provided a reference voltage between 0.0 and ± 1.0 volts. These voltages were applied through the Universal Bridge in the capacitance mode between the working Fe_2O_3 and the counter carbon electrodes. The voltages applied to the working electrode were converted to voltages with respect to the reference SCE electrode by switching in the microvoltmeter prior to measuring the capacitance, measuring the voltage with respect to the SCE electrode and then switching out the microvoltmeter to measure the capacitance of the working electrode.

The electrolyte contact to the Fe_2O_3 pellets was, in all experiments, prepared with 0.1M K_2SO_4 as the supporting electrolyte and was either buffered at pH 4.01, 7.00, 10.00 with Mallinckrodt AR buffer solutions or prepared at unbuffered pH 6.75 and 14.00 by adjusting the 0.1M K_2SO_4 solution with sodium hydroxide. All chemicals were AR grade and all measurements of the photocurrents were carried at 295 K. All photocurrents were steady state measurements.

Resistivities of the sintered Fe_2O_3 pellets were measured by DC and AC resistance probes, the two results agreeing within experimental error.

RESULTS AND DISCUSSION

a) Resistivity Measurements

Sintered polycrystalline pellets of Fe_2O_3 have large resistivities at room temperature and are basically intrinsic semiconductors with a band gap of approximately 2.0 eV. Like other intrinsic semiconductors, the electrical properties can be modified by doping the semiconductor with either electron donors (n-type impurities) or electron acceptors (p-type impurities). Titanium dioxide powder, when mixed with the Fe_2O_3 powder and subsequently pressed and sintered, enters the $\alpha\text{-Fe}_2\text{O}_3$ lattice substitutionally as Ti^{+4} resulting in an Fe^{+3} Fe^{+2} charge transfer to maintain charge neutrality in the bulk semiconductor. The effect was first reported by Verwey¹⁸ and more recently applied to Fe_2O_3 by Morin¹⁷ to produce n-type semiconducting material. It was shown that increasing amounts of Ti atoms produce lower resistivities at room temperature.

Using a technique similar to that used by Morin (see experimental section), pellets were made with resistivities from approximately $1000\Omega\text{-cm}$ to $10^{10}\Omega\text{-cm}$. Low concentrations (less than 0.1 at.%) of Ti affect the resistivity the greatest while concentrations greater than 0.5 at.% Ti have no effect

on the resistivity, the resistivity leveling off at $700\Omega\text{-cm}$ for at.% Ti 0.5. In all subsequent work, resistivities of $700\Omega\text{-cm}$ are used corresponding to 1.0 at.% Ti.

b) Capacitance Measurements

Varying the voltage between the working electrode and the counter electrode results in a change in capacitance of the working electrode and when plotted as a Mott-Schottky relation¹⁶ (eqn. 1), a straight line is obtained at all pH in the range 4 - 14 (Fig. 2)

$$d(1/C^2)/dU = 2/q \epsilon \epsilon_0 N_D \quad (1)$$

where C is the capacitance (F cm^{-2}) in the space charge region of the semiconductor showing that other capacitance due to the Helmholtz and Gouy layers and any charged surface states must be too large to be important. U is the applied voltage (volts) with respect to the SCE, q the electronic charge (C), ϵ_0 the permittivity of free space (F cm^{-1}), ϵ the relative dielectric constant of the Fe_2O_3 semiconductor in the space charge region and N_D the donor density (cm^{-3}). Since the real surface area of the polycrystalline sintered pellet is unknown, N_D cannot be obtained from the Mott-Schottky slope.

The flat band potential of the semiconductor at a given pH is obtained, however, by extrapolating to zero on the $1/C^2$ axis. Values of the flat band potentials at various pH are shown in Table 1 and the effect of the pH shown graphically in Fig. 3. The slope of the straight line fit to the data obtained from a linear least squares analysis is approximately 56 mV/pH unit indicating that the surface of the polycrystalline Fe_2O_3 sintered semiconductor is chemically stable under the conditions applied here¹⁹.

Table 1 summarizes the data obtained both here on the polycrystalline

sintered Fe_2O_3 and that on thin films¹⁵ and single crystals⁵. The data for the voltage at which the onset of the photocurrent is seen to occur is, in an ideal case, equal to the flat band potential. The discrepancy between the two sets of data is not explicable at present. Nevertheless, the results obtained on the different types of semiconductor are in reasonably good agreement at alkaline pH while at acidic pH a significant discrepancy between the thick film and sintered pellet data is observed. Unfortunately, no single crystal data was available for comparison at low pH. It should be noted that the thin films showed instability at pH of 4 while no degradation of the semiconductor could be observed, the photocurrents becoming steady after the typical initial decay (see next section). Possibly the method of preparation of the thin films of Fe_2O_3 made the thin films more amenable to acid degradation since thin films of Fe_2O_3 prepared by different techniques have been shown to be stable even at a pH of 4⁹. As further evidence of the stability of the polycrystalline sintered Fe_2O_3 at pH of 4, it can be seen in Fig. 3 that the flat band potential estimated from the capacitance measurements at a pH of 4 lies on the straight line connecting the flat band potentials measured at higher pH. Degradation of the semiconductor surface is indicated in such plots of flat band potentials versus pH by a strong deviation from the straight line at values of the pH where the degradation occurs. This effect is related to the protonation of the oxide semiconductor surface when in contact with an electrolyte and the resulting changes in the charge distribution in the space charge region of the semiconductor associated with this extra adsorbed charge. Variation of the electrolyte pH changes the protonation of the semiconductor surface which in turn results in an approximate 60 mV/pH unit change in flat band potential. Any degradation of the semiconductor surface will result in a new surface which, in all probability, will not accumulate protons with an identical capacity to the undamaged surface

and so will not change the flat band potential by the normal 60 mV/pH unit.

No capacitance measurements on the thin films were reported so that estimates of the flat band potential were only available from the data on the voltage onset of the photocurrent. As can be seen in Table 1, a large discrepancy between the onset voltage and the flat band potential exist in both the polycrystalline and single crystal Fe_2O_3 .

c) Photoelectrochemistry

Steady state photocurrents were recorded after the initial anodic photocurrent transient, observed with monochromatic irradiation, decayed after several minutes. A cathodic photocurrent transient lasting seconds also was observed with thin film Fe_2O_3 and can be seen with polycrystalline sintered pellets upon the removal of the radiation. As with thin films, the transients (cathodic⁶ and anodic^{6,9}) merge into the photocurrent itself at high intensity white light irradiation. The postulate⁶ of a light intensity-independent back reaction competing at low level monochromatic irradiations with the forward electron injection into the conduction band would require a high density of surface states at which the back reaction could occur and which are only significant in the back reaction. Having no effect on the forward reaction, the surface states do not influence the capacitance measurements allowing a linear Mott-Schottky effect to be observed. This is not unreasonable on polycrystalline thin film and sintered pellets. However, the effect might be expected to be reduced on a clean single crystal surface. No results on the transient effects on single crystals were available. Nevertheless, the photocurrent increases linearly with the irradiance at all wavelengths studied.

The polycrystalline sintered Fe_2O_3 electrodes showed sizeable dark currents at low applied voltages (+0.2 v. SCE; $7.6 \times 10^{-7} \text{ A cm}^{-2}$) which

increased rapidly at anodic voltages greater than +1.0 v.SCE. The presence of both surface states and grain boundaries at the surface of the polycrystalline Fe_2O_3 inhibited the formation of a true depletion layer characterized in the single crystal Fe_2O_3 by no large dark currents even at applied voltages of +5.0 v.SCE and a saturation in the photocurrent versus applied voltage response⁵. A degree of saturation can be seen in the photocurrent - applied voltage response curves (Fig. 4) of the polycrystalline sintered Fe_2O_3 . The sintered pellet lies intermediate between the polycrystalline thin films^{6,9} and the single crystal.⁵ A plot of efficiency (electron/incident photon) versus wavelength at pH 6.75 is shown in Fig. 5, the onset of the photo-effect occurring near 600 nm corresponding to a band gap of approximately 2.1 eV.^{5,6}

Going from acidic to alkaline pH results in a cathodic shift in the onset voltage of the photocurrent and a plot of V_{on} versus pH results in a straight line with a slope of approximately 60 mV/pH unit. Similar work on TiO_2 single crystal electrodes gave also a slope of 60 mV/pH unit attributable to the presence of the protonated semiconductor surface layer.¹⁹

Using a value²⁰ of $0.1 \text{ cm}^2\text{V}^{-1} \text{ s}^{-1}$ for the mobility of the electron in Ti doped n-type Fe_2O_3 and a value of $700\Omega\text{-cm}$ for the resistivity (1.0 at.% Ti), the ionized donor density (Ti^{+4}) can be calculated to be $8 \times 10^{16} \text{ cm}^{-3}$. Using this approximate value for N_D and the Mott-Schottky relation (eqn. 1), the real surface area of the polycrystalline sintered Fe_2O_3 pellet is 1.04 cm^2 which gives a real to apparent surface area of 15. In the calculation of this value, the value of 120 was used for the relative dielectric constant of Fe_2O_3 ⁵. Thus, although the real surface area is larger than the apparent surface area for a polycrystalline sintered Fe_2O_3 , little more can be drawn from these numbers due to the large

uncertainties in the mobility and the dielectric constant.

CONCLUSION

Iron oxide can be formed into n-type semiconductor by doping with Ti atoms and sintering the pellet to obtain a polycrystalline semiconductor intermediate in properties between the polycrystalline thin film^{6,9} and the single crystal⁵. The net photocurrent saturates with increasing anodic polarization due to the depletion layer formed at the semiconductor electrolyte interface even though large dark currents are observable at as little as 1.0 v.SCE. The photocurrent onset occurs at increasingly cathodic potentials with more alkaline pH with a flat band potential of -0.6 v. SCE at pH of 14, typical of most oxide semiconductors. Thus, even though the spectral response of the Fe_2O_3 is a fairly good match with the solar spectrum, the flat band potential is insufficiently negative (less than -1.20 v.SCE) to be able to produce hydrogen from water even though stable oxygen evolution is observed.²¹ To act in a self-sufficient solar cell, therefore, it must be combined with a stable p-type photocathode. We are, at present, conducting research in this area.

ACKNOWLEDGEMENTS

The author wishes to thank Dr. Mark Spitler and Mr. Terje Skotheim for their knowledge and skills in semiconductor electrochemistry and physics which they passed on to me in such an enjoyable atmosphere.

This work was supported by the Basic Energy Sciences Division of the Department of Energy.

REFERENCES

- ¹A. Fujishima, K. Kohayakawa, and K. Honda, *J. Electrochem. Soc.* 122,(11), 1487 (1975).
 - ²M. S. Wrighton, A. B. Ellis, P. T. Wolczanski, D. L. Morse, H. B. Abrahamson, and D. S. Ginley, *J. Amer. Chem. Soc.* 98(10), 2774 (1976).
 - ³J. G. Mavroides, J. A. Kafalas, and D. F. Kolesar, *Appl. Phys. Lett.* 28(5), 241 (1976).
 - ⁴G. Hodes, D. Cahen, and J. Manassen, *Nature* 260, 312 (1976).
 - ⁵R. K. Quinn, R. D. Nasby, and R. J. Baughman, *Mat. Res. Bull.* 11, 1011 (1976).
 - ⁶K. L. Hardee and A. J. Bard, *J. Electrochem. Soc.* 124(2), 215 (1977).
 - ⁷H. H. Kung, H. S. Jarrett, A. W. Sleight, and A. Ferretti, *J. Appl. Phys.* 48(6), 2463 (1977).
 - ⁸D. S. Ginley and M. A. Butler, *J. Appl. Phys.* 48(5), 2019 (1977).
 - ⁹Lun-Shu Ray Yeh and N. Hackerman, *J. Electrochem. Soc.* 124(6), 833 (1977).
 - ¹⁰M. A. Butler and D. S. Ginley, *J. Appl. Phys.* 48(7), 3070 (1977).
 - ¹¹J. Augustynski, J. Hinden, and Chs. Stadler, *J. Electrochem. Soc.* 124(7), 1063 (1977).
 - ¹²A. Fujishima, K. Kohayakawa, and K. Honda, *Bull. Chem. Soc. Japan*, 48(3), 1041 (1975).
 - ¹³M. S. Wrighton, D. S. Ginley, P. T. Wolczanski, A. B. Ellis, D. L. Morse, and A. Linz, *Proc. Nat. Acad. Sci.* 72(4), 1518 (1975).
 - ¹⁴T. Watanabe, A. Fujishima, and K. Honda, *Bull. Chem. Soc. Japan*, 49(2), 355 (1976).
-

- ¹⁵K. Hardee and A. J. Bard, J. Electrochem. Soc. 123(7), 1024 (1976).
- ¹⁶H. Gerischer, Adv. Electrochem. Electrochem. Engng. 1, C. Tobias and P. Delahay, eds. (Interscience, 1961).
- ¹⁷F. J. Morin, Phys. Rev. 83(5), 1005 (1951).
- ¹⁸E. J. W. Verwey, P. W. Haaijman, F. C. Romeijn, and G. W. van Oosterhout, Phillips Res. Repts. 5, 173 (1950).
- ¹⁹A. Fujishima, A. Sakamoto, and K. Honda, Seisan Kenkyu, 21(7), 450 (1969).
- ²⁰A. J. Bosman and H. J. van Daal, Adv. in Phys. 19, 1 (1970).
- ²¹J. G. Mavroides, D. I. Tchernov, J. A. Kafalas, and D. F. Kolesar, Mat. Res. Bull. 10, 1023 (1975).

LIST OF CAPTIONS

Fig. 1. Experimental Equipment for measuring Photoelectrochemical Properties of a Working Electrode.

Fig. 2. Applied Voltage Effects on the Capacitance of the Fe_2O_3 - Electrolyte Interface measured at a frequency of 1 kHz. Electrolyte 0.1 M K_2SO_4 at a pH of ●, 4.01 (buffered); ○, 10.00 (buffered); x, 14.00 (not buffered).

Fig. 3. Hydrogen Ion Concentration Effect on the Flat Band Potential (E_{FB}) and the Onset Voltage (V_{ON}) in 0.1 M K_2SO_4 .

Fig. 4. Efficiency of Free Electron Formation per Incident Photon as a function of Applied Voltage at 0.1 M K_2SO_4 and pH of 6.75. Wavelength of the incident radiation ●, 540 nm; ○, 500 nm; x, 440 nm.

Fig. 5. Photoaction Spectrum of Fe_2O_3 in 0.1 M K_2SO_4 at a pH of 6.75 at different applied voltages vs. SCE ●, + 1.0 v.SCE; ○, + 0.7 v.SCE; x, + 0.5 v.SCE.

TABLE 1

Comparison of Onset Voltage and Flat Band Potentials
 Obtained on Thin Films (I), Single Crystals (II),
 and Polycrystalline Sintered Pellets (III).

pH	V_{on} (v.SCE)			E_{FB} (v.SCE)		
	I ¹⁵	II ⁵	III	I	II	III
4.00	+0.4		+0.2			-0.06
4.50						
6.30		+0.23			-0.1	
6.70	+0.2	+0.22	0.0		-0.1	-0.2
8.60		+0.12			-0.41	
10.00	-0.2		-0.2			-0.4
14.0	-0.4	-0.36	-0.4		-0.67	-0.6

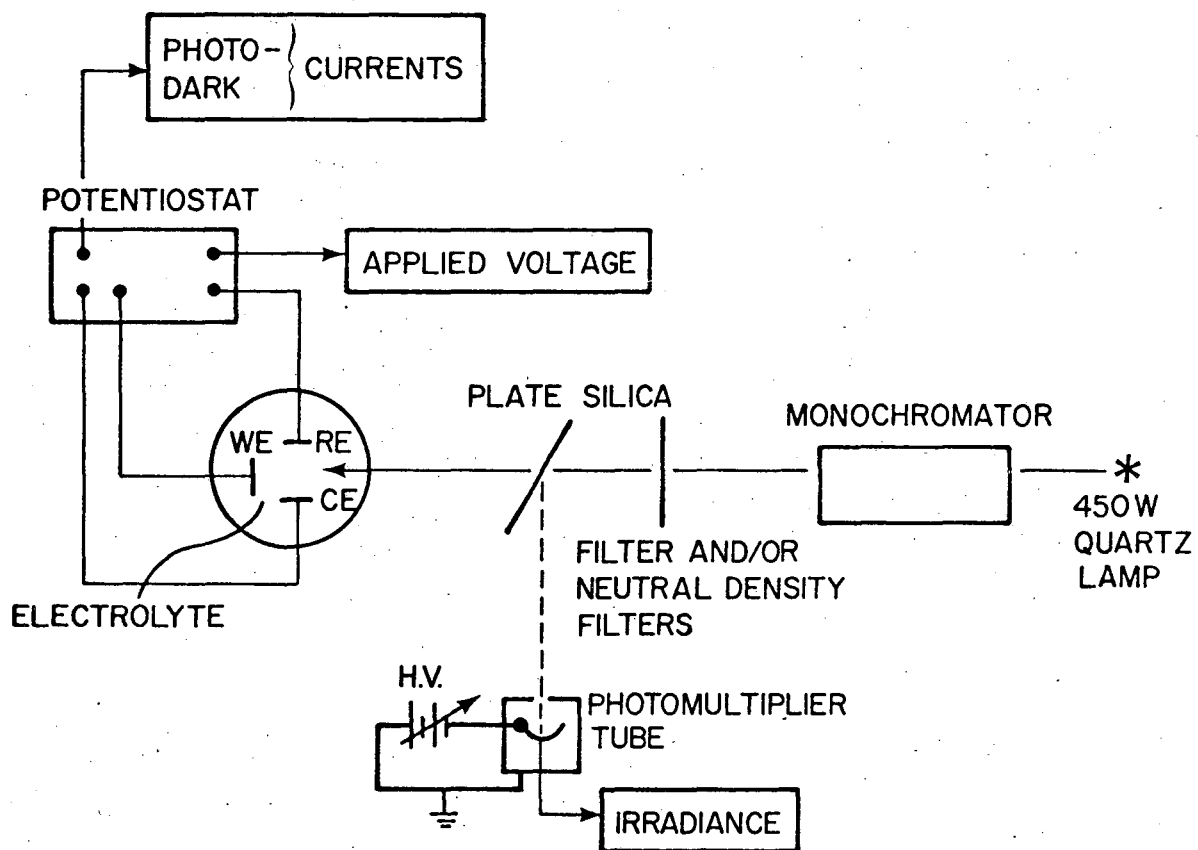
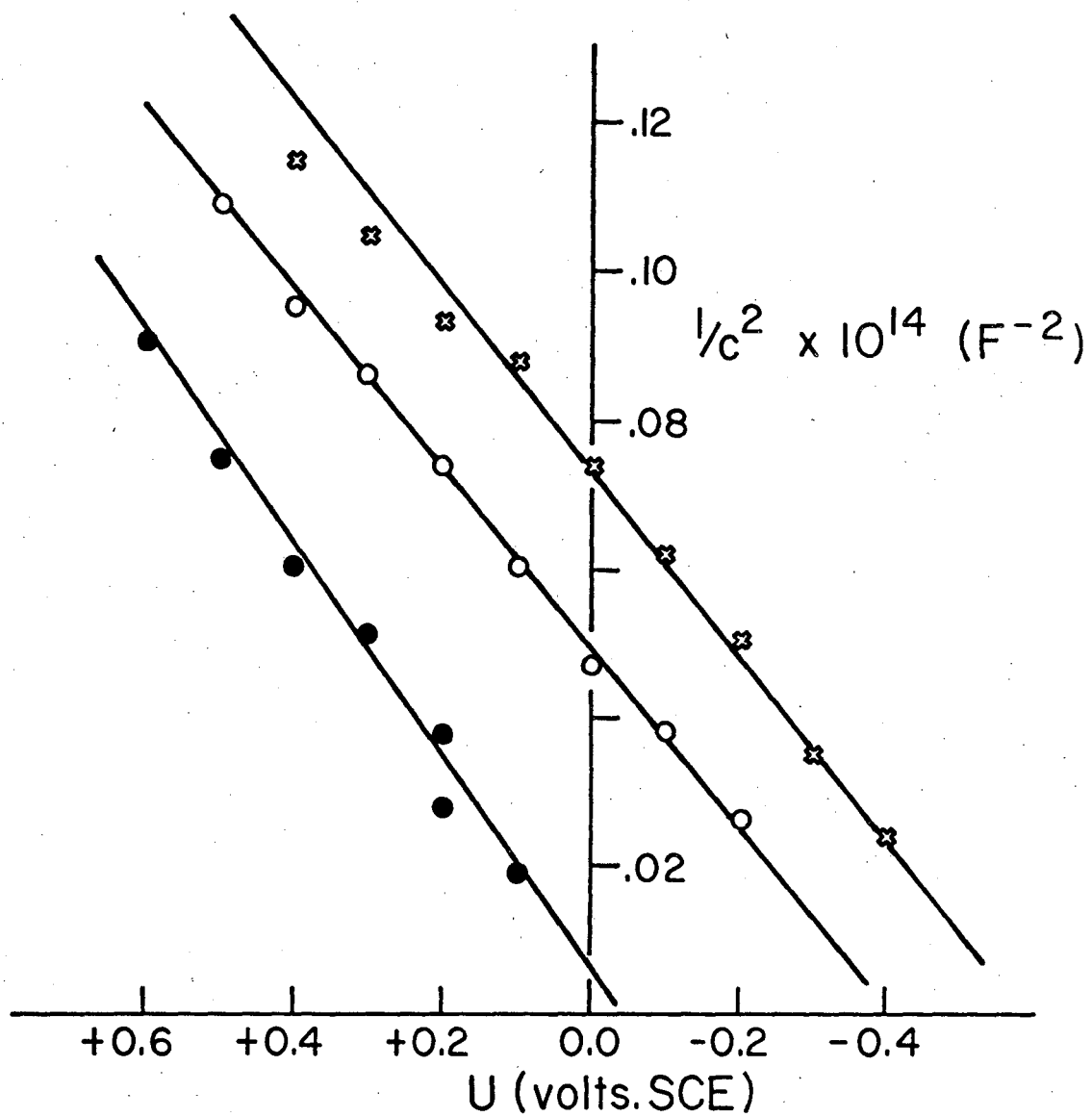
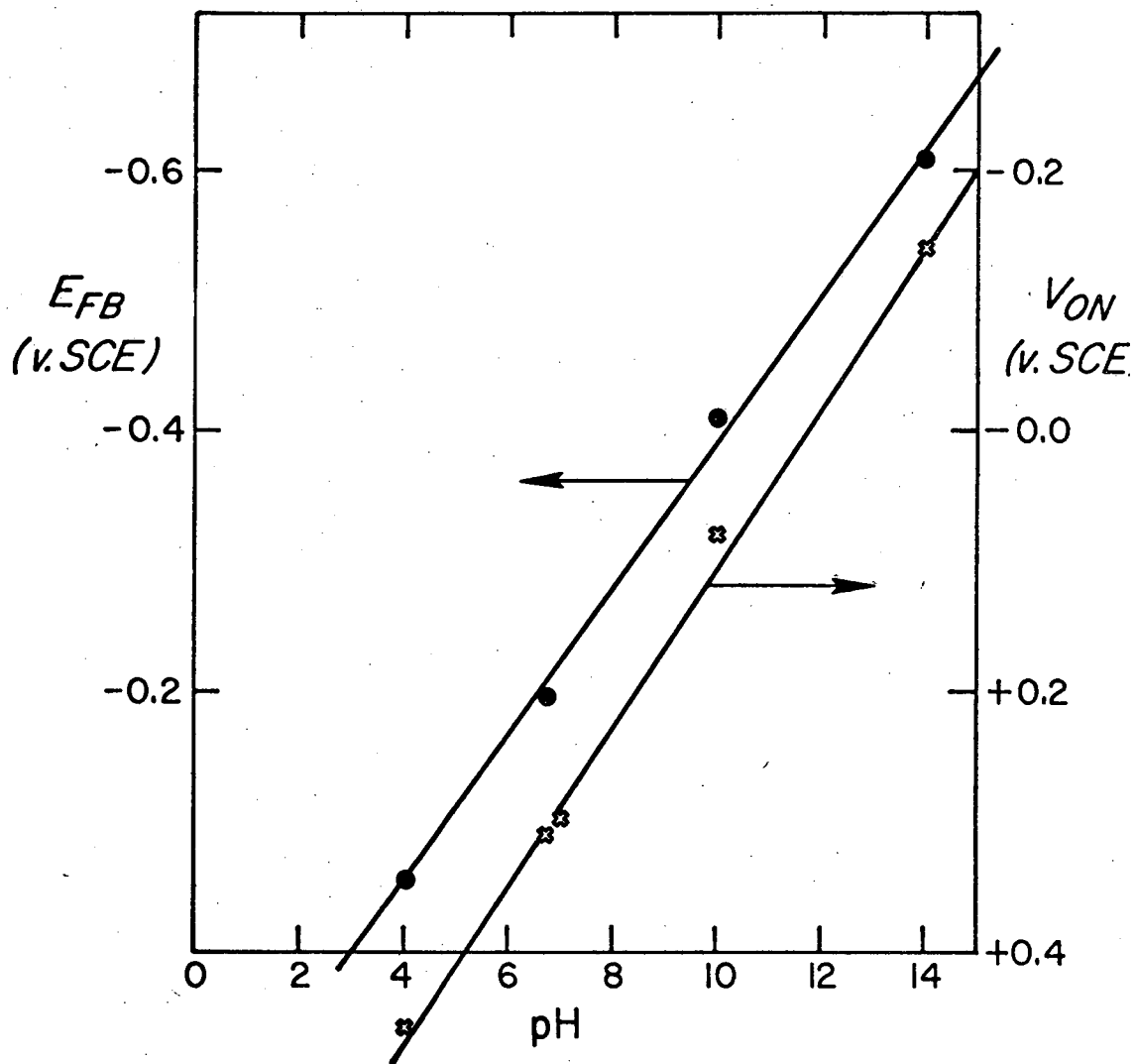


Fig. 1



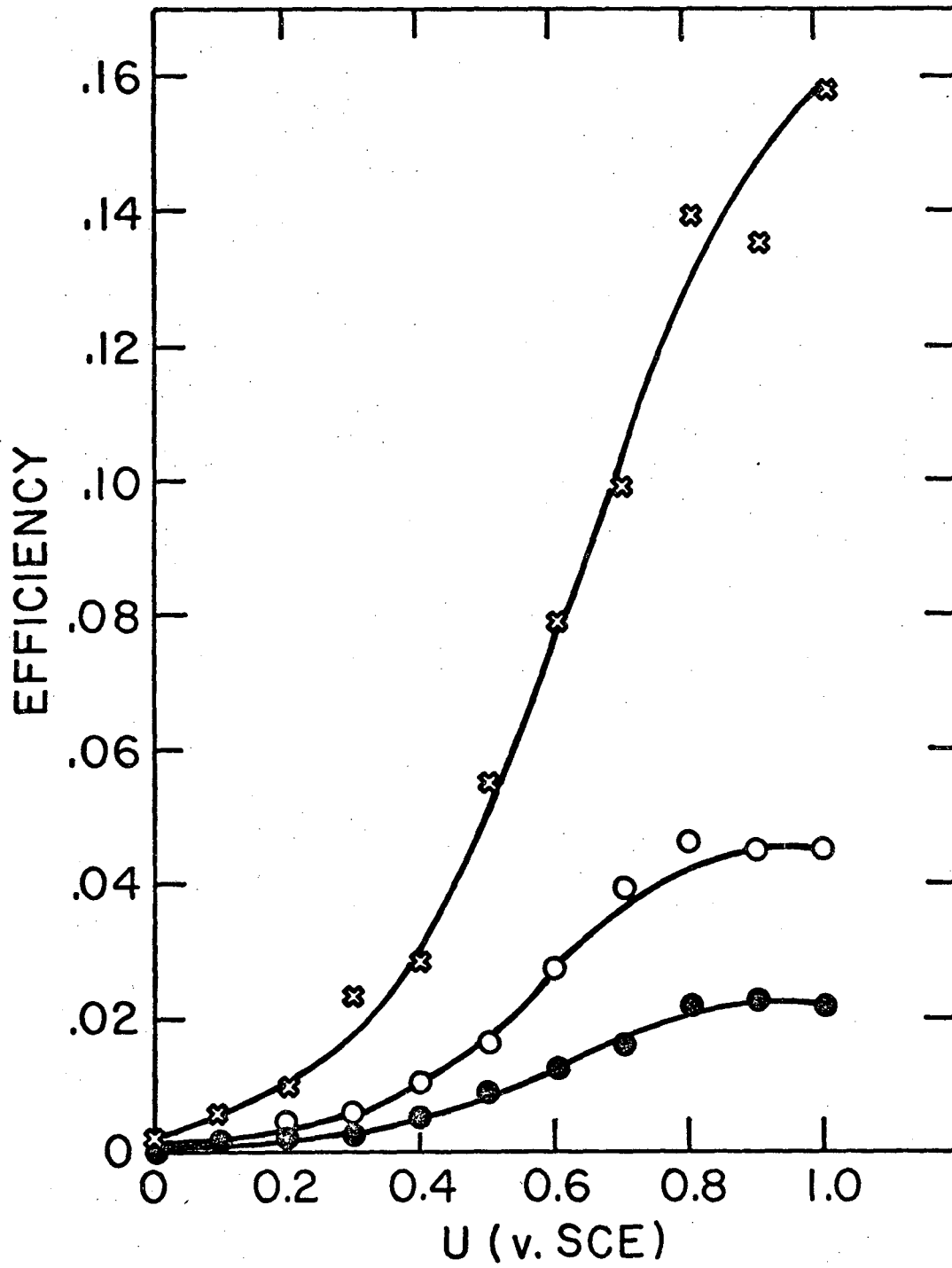
XBL 781-3774

Fig. 2



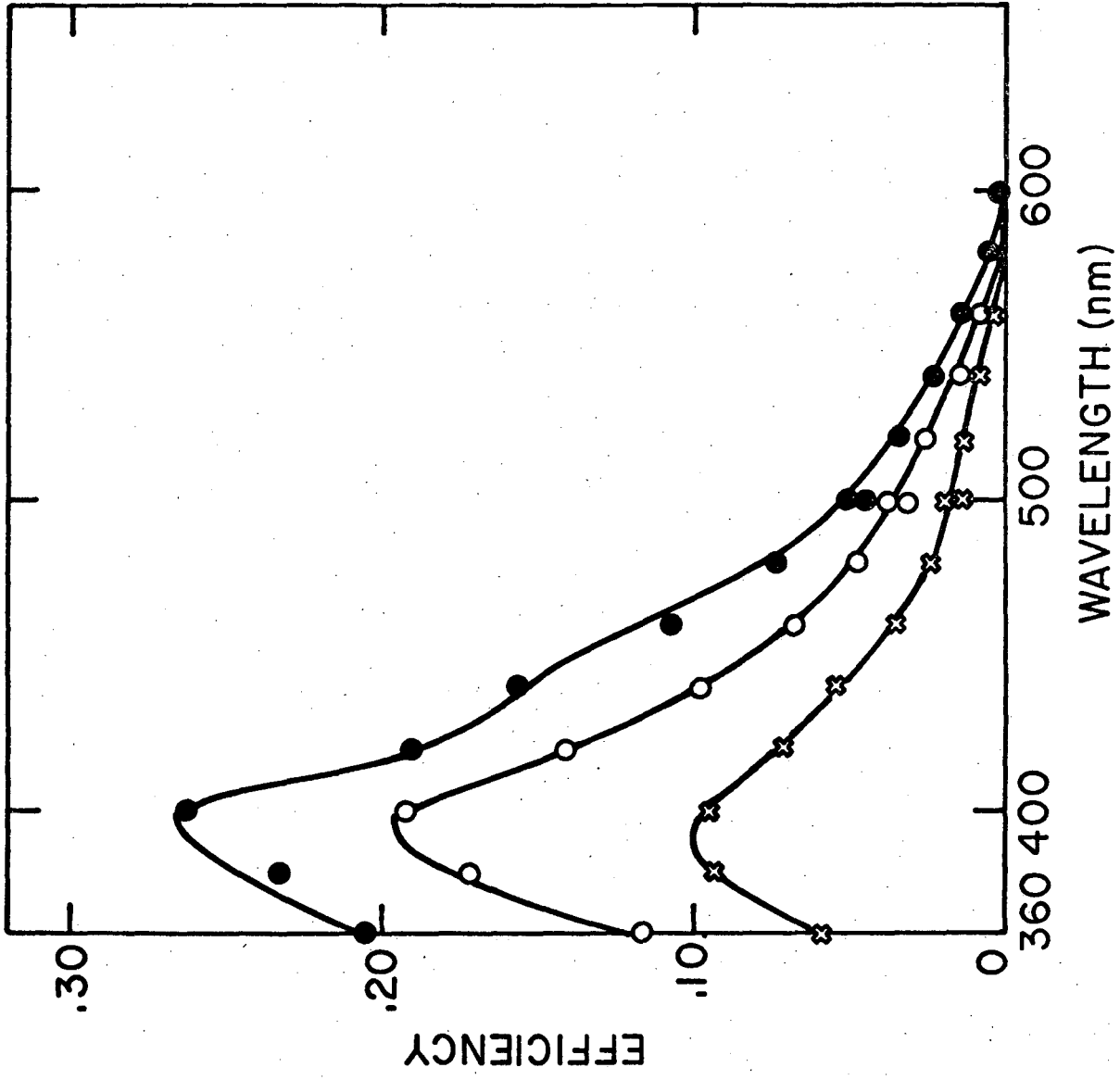
XBL 781-3773

Fig. 3



XBL 781-3772

Fig. 4



XBL 781-3771

Fig. 5

This report was done with support from the Department of Energy. Any conclusions or opinions expressed in this report represent solely those of the author(s) and not necessarily those of The Regents of the University of California, the Lawrence Berkeley Laboratory or the Department of Energy.

TECHNICAL INFORMATION DEPARTMENT
LAWRENCE BERKELEY LABORATORY
UNIVERSITY OF CALIFORNIA
BERKELEY, CALIFORNIA 94720